

Supporting Information

Highly stable CsPbBr₃ perovskite phases from new lead β -diketonate glyme adducts

Lorenzo Sirna,^a Anna L. Pellegrino,^{a,*} Salvatore P. Sciacca,^a Martina Lippi,^b Patrizia Rossi,^b Carmela Bonaccorso,^c Giuseppe Bengasi,^d Marina Foti,^d Graziella Malandrino^{a,*}

^a Dipartimento Scienze Chimiche, Università degli Studi di Catania, and INSTM UdR Catania, Viale Andrea Doria 6, 95125 Catania, Italy

^b Dipartimento di Ingegneria Industriale, Università di Firenze, Via Santa Marta 3, 50136 Firenze, Italy

^c Dipartimento Scienze Chimiche, Università degli Studi di Catania, Viale Andrea Doria 6, 95125 Catania, Italy

^d 3SUN s.r.l., Contrada Blocco Torrazze, 95121, Catania, Italy

Corresponding: annalucia.pellegrino@unict.it, graziella.malandrino@unict.it

Table of contents

Fig. S1. Ball and stick view of the two independent molecules of Pb(hfa)₂•monoglyme.

Fig. S2. Superimposition of the two independent Pb (II) complexes in Pb(hfa)₂•monoglyme.

Table S1. Selected bond lengths and angles in Pb(hfa)₂monoglyme.

Fig. S3. ¹H NMR spectra of the Pb(hfa)₂•glyme complexes 1-4.

Fig. S4. ¹³C NMR spectra of the Pb(hfa)₂•glyme complexes 1-4.

Fig. S5. ¹³C-NMR signals for the CF₃ and CO groups of the Pb(hfa)₂•glyme complexes 1-4.

Fig S6. EDX Spectrum and quantitative analysis of the TGA residue of [Pb(hfa)₂•triglyme•H₂O].

Fig S7. ATR-IR spectra of **CsPbBr₃_1**, **CsPbBr₃_2**, **CsPbBr₃_3** and **CsPbBr₃_4** microcrystals.

Fig S8. TGA curves of **CsPbBr₃_1**, **CsPbBr₃_2**, **CsPbBr₃_3** and **CsPbBr₃_4** microcrystals.

Fig S9. EDX Spectrum and quantitative analysis of **CsPbBr₃_1**.

Fig S10. EDX Spectrum and quantitative analysis of **CsPbBr₃_2**.

Fig S11. EDX Spectrum and quantitative analysis of **CsPbBr₃_3**.

Fig S12. EDX Spectrum and quantitative analysis of **CsPbBr₃_4**.

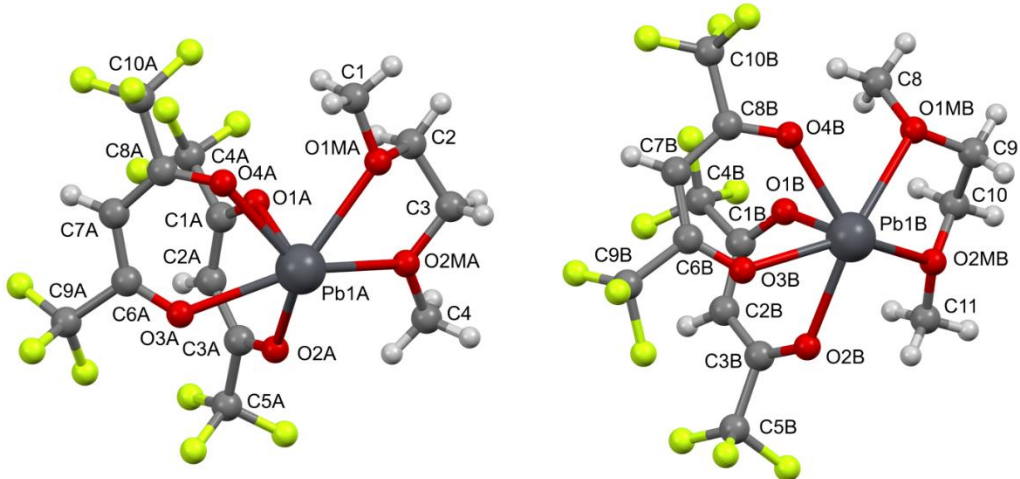


Fig. S1. Ball and stick view of the two independent molecules of $\text{Pb}(\text{hfa})_2 \bullet \text{monoglyme}$ showing the atom labelling for the Pb, O and C atoms. For the sake of clarity only one model was reported for the disordered moieties.

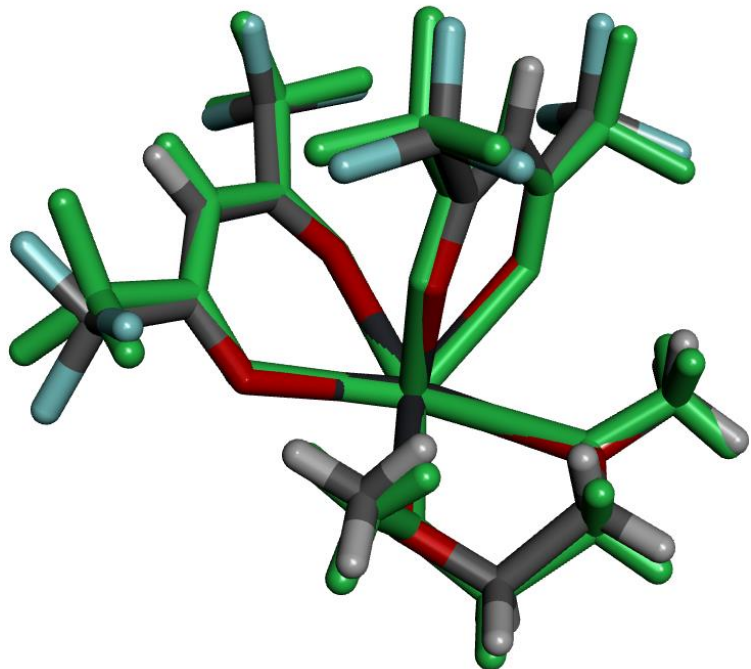


Fig. S2. Superimposition of the two independent Pb (II) complexes in $\text{Pb}(\text{hfa})_2 \bullet \text{monoglyme}$. (stick, color by elements: Pb1A complex; stick, pale green: Pb1B complex)

Table S1. Selected bond lengths (\AA) and angles ($^\circ$) in **Pb(hfa)₂monoglyme**.

Pb-X			
Pb1A-O1A	2.369(6)	Pb1B-O1B	2.347(5)
Pb1A-O2A	2.509(4)	Pb1B-O2B	2.523(5)
Pb1A-O3A	2.546(5)	Pb1B-O3B	2.476(5)
Pb1A-O4A	2.509(5)	Pb1B-O4B	2.466(4)
Pb1A-O1MA	2.620(5)	Pb1B-O1MB	2.729(6)
Pb1A-O2MA	2.665(6)	Pb1B-O2MB	2.738(5)
Pb1A ¹ -Pb1A ¹	3.8012(5)	Pb1B ¹ -Pb1B ²	3.9518(6)
X-Pb-Y			
O1A-Pb1A-O2A	73.5(2)	O1B-Pb1B-O2B	73.6(2)
O1A-Pb1A-O3A	81.0(2)	O1B-Pb1B-O3B	82.7(2)
O1A-Pb1A-O4A	72.6(2)	O1B-Pb1B-O4B	74.9(2)
O1A-Pb1A-O1MA	79.5(2)	O1B-Pb1B-O1MB	76.4(2)
O1A-Pb1A-O2MA	78.8(2)	O1B-Pb1B-O2MB	76.3(2)
O2A-Pb1A-O3A	65.8(2)	O2B-Pb1B-O3B	66.3(2)
O2A-Pb1A-O4A	127.5(2)	O2B-Pb1B-O4B	129.6(2)
O2A-Pb1A-O1MA	132.7(2)	O2B-Pb1B-O1MB	134.7(1)
O2A-Pb1A-O2MA	73.6(2)	O2B-Pb1B-O2MB	77.3(2)
O3A-Pb1A-O4A	70.3(2)	O3B-Pb1B-O4B	71.5(2)
O3A-Pb1A-O1MA	146.1(2)	O3B-Pb1B-O1MB	141.1(1)
O3A-Pb1A-O2MA	138.3(2)	O3B-Pb1B-O2MB	141.9(2)
O4A-Pb1A-O1MA	77.5(2)	O4B-Pb1B-O1MB	71.5(1)
O4A-Pb1A-O2MA	134.9(2)	O4B-Pb1AB-O2MB	130.5(2)
O1MA-Pb1A-O2MA	63.3(2)	O1MB-Pb1B-O2MB	63.1(2)

¹ = -x, -y, 1-z; ² = 1-x, 1-y, -z

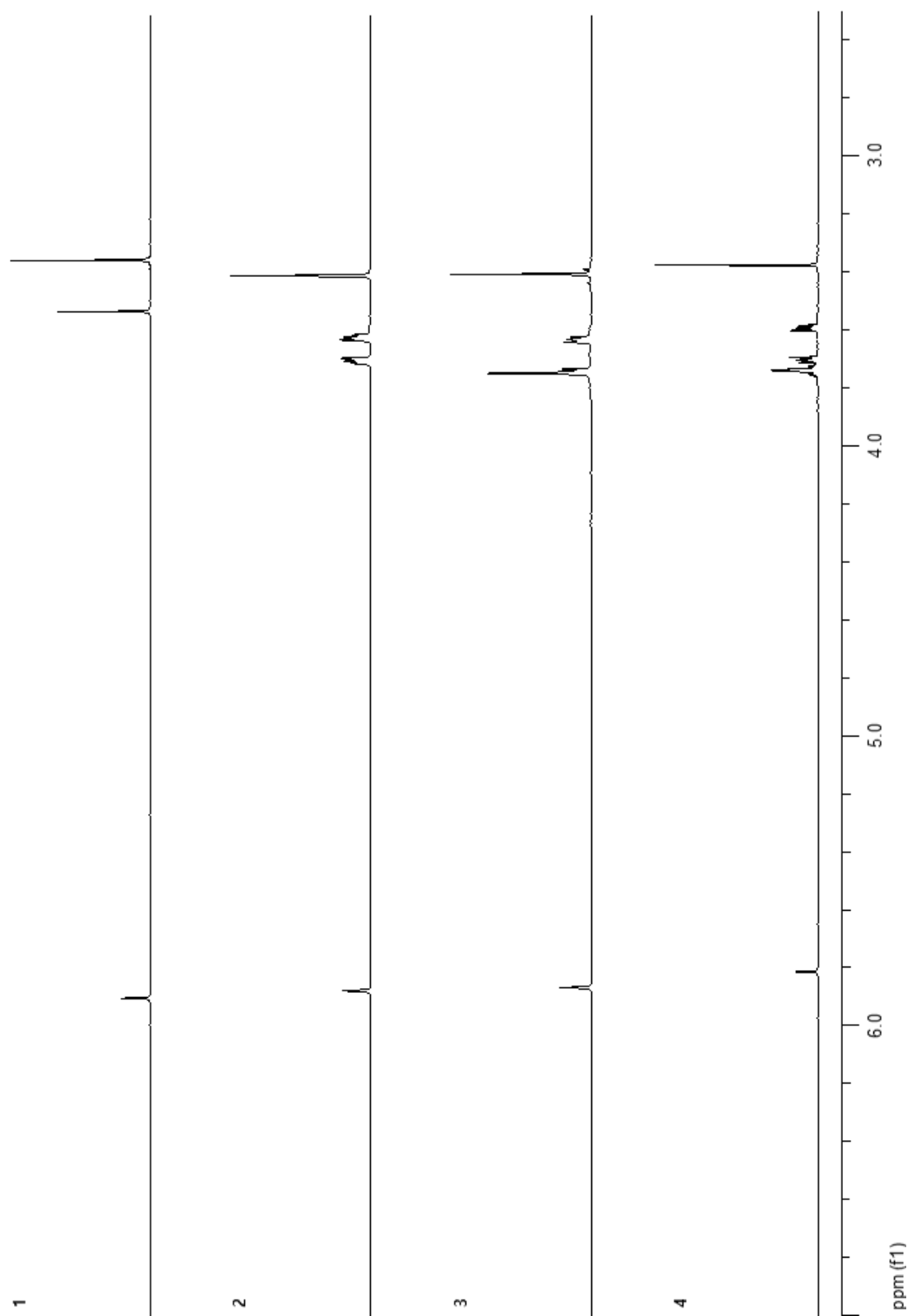


Fig. S3. ¹H NMR spectra of the Pb(hfa)₂•glyme complexes 1-4 (CD₃CN, 500 MHz, 27 °C).

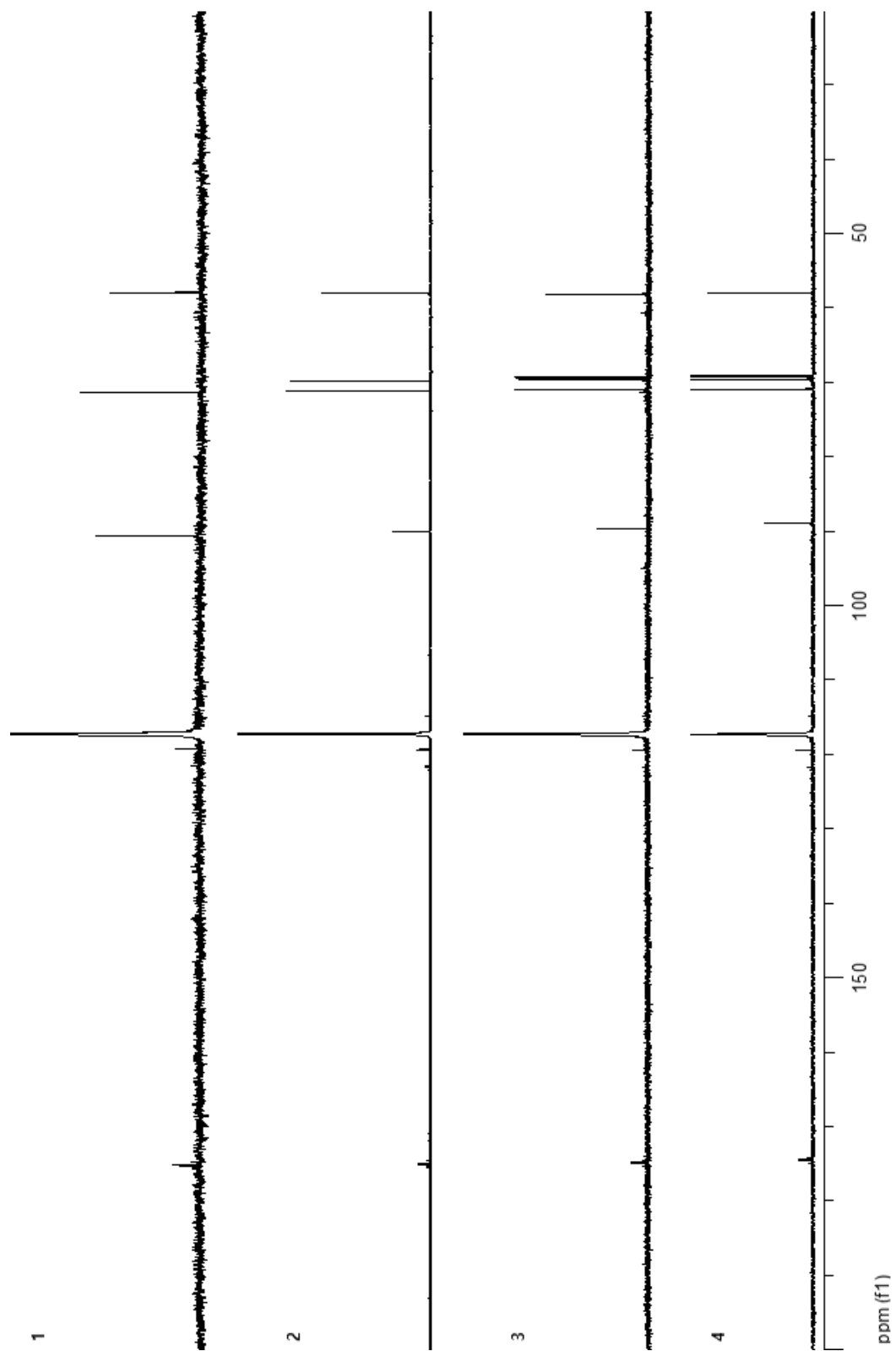


Fig. S4. ^{13}C NMR spectra of the $\text{Pb}(\text{hfa})_2 \bullet \text{glyme}$ complexes 1-4 (CD_3CN , 125 MHz, 27 °C).

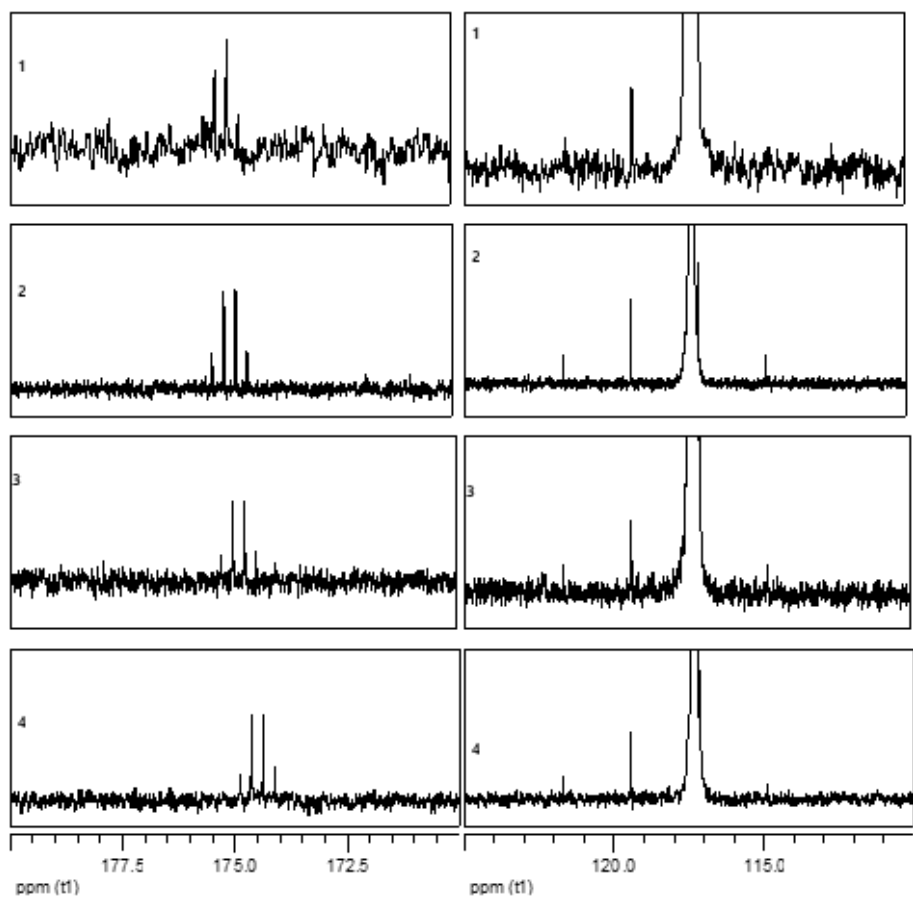


Fig. S5. ^{13}C -NMR signals for the CF_3 and CO groups of the $\text{Pb}(\text{hfa})_2\bullet\text{glyme}$ complexes 1-4 (CD_3CN , 125 MHz, 27 °C).

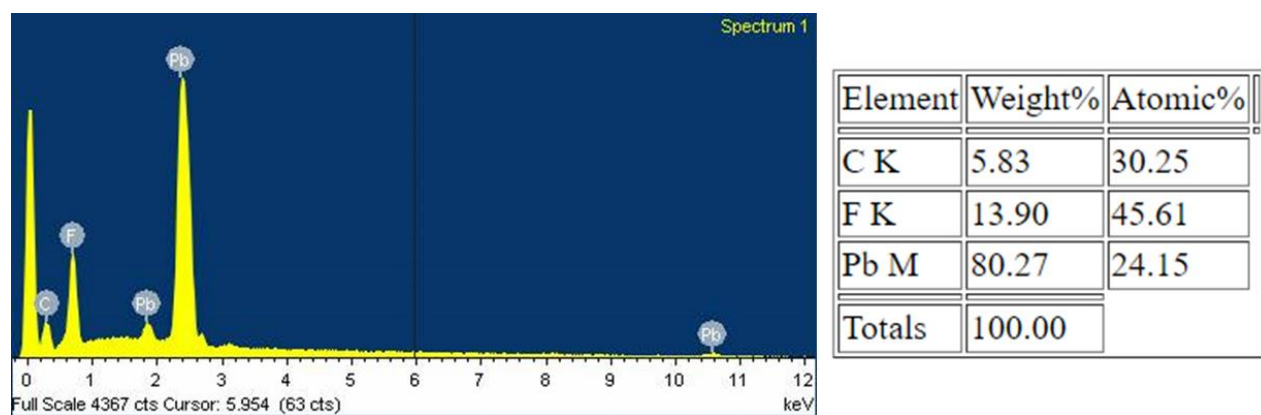


Fig S6. EDX Spectrum of TGA residue of $[\text{Pb}(\text{hfa})_2\bullet\text{triglyme}\bullet\text{H}_2\text{O}]$ and quantitative analysis of the residue.

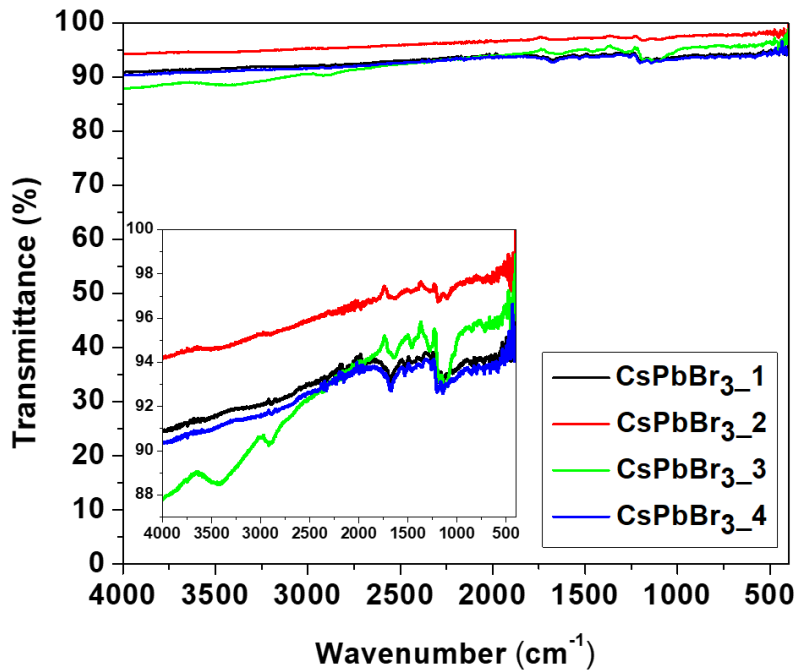


Fig S7. ATR-IR spectra of $\text{CsPbBr}_3\text{-1}$, $\text{CsPbBr}_3\text{-2}$, $\text{CsPbBr}_3\text{-3}$ and $\text{CsPbBr}_3\text{-4}$ microcrystals.

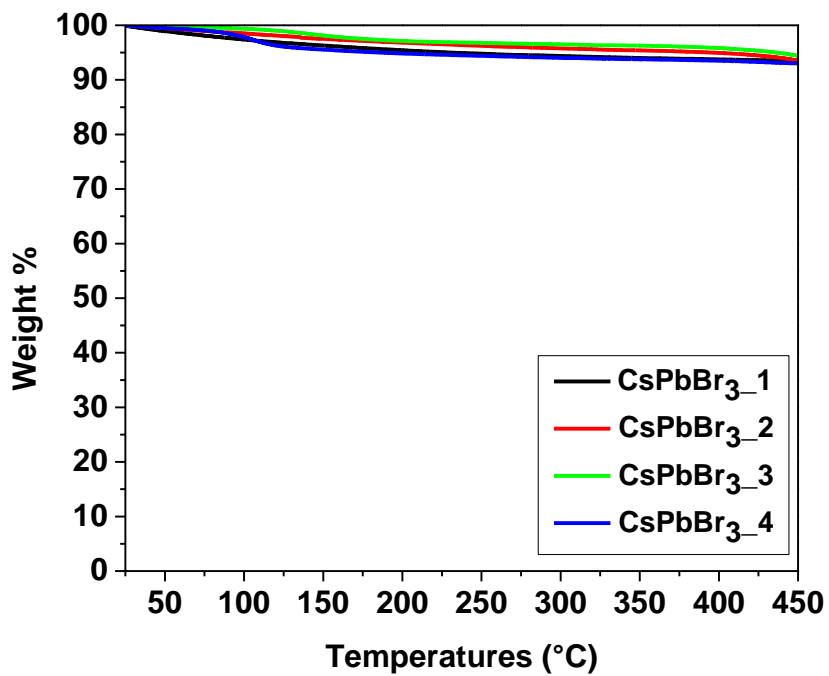


Fig S8. TGA curves of $\text{CsPbBr}_3\text{-1}$, $\text{CsPbBr}_3\text{-2}$, $\text{CsPbBr}_3\text{-3}$ and $\text{CsPbBr}_3\text{-4}$ microcrystals.

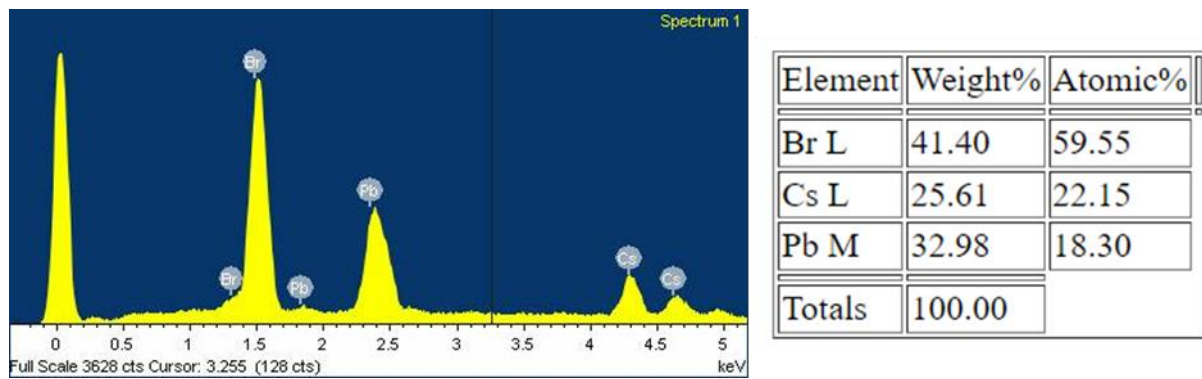


Fig S9. EDX Spectrum of $\text{CsPbBr}_3\text{-1}$ and quantitative analysis of the powder.

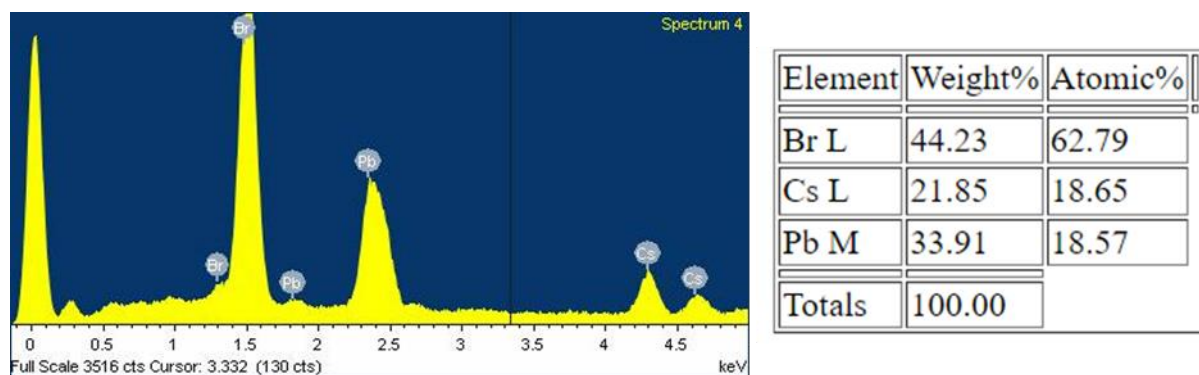


Fig S10. EDX Spectrum of $\text{CsPbBr}_3\text{-2}$ and quantitative analysis of the powder.

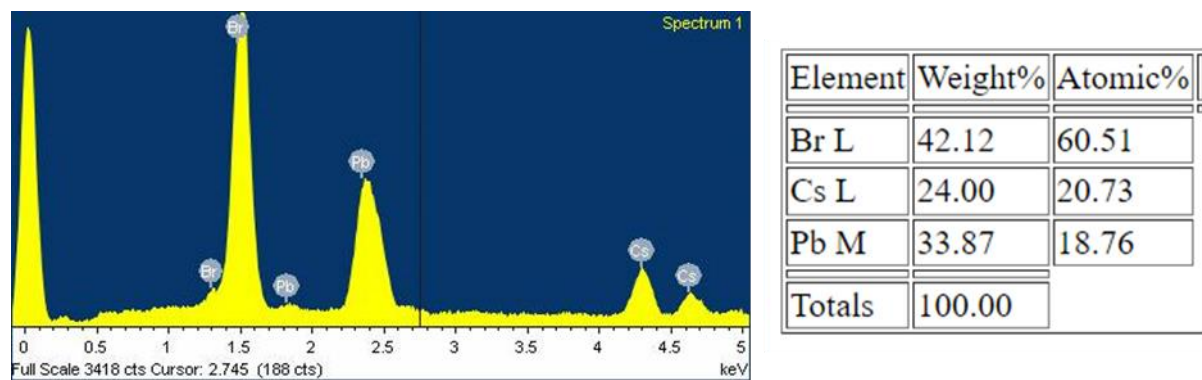


Fig S11. EDX Spectrum of $\text{CsPbBr}_3\text{-}3$ and quantitative analysis of the powder.

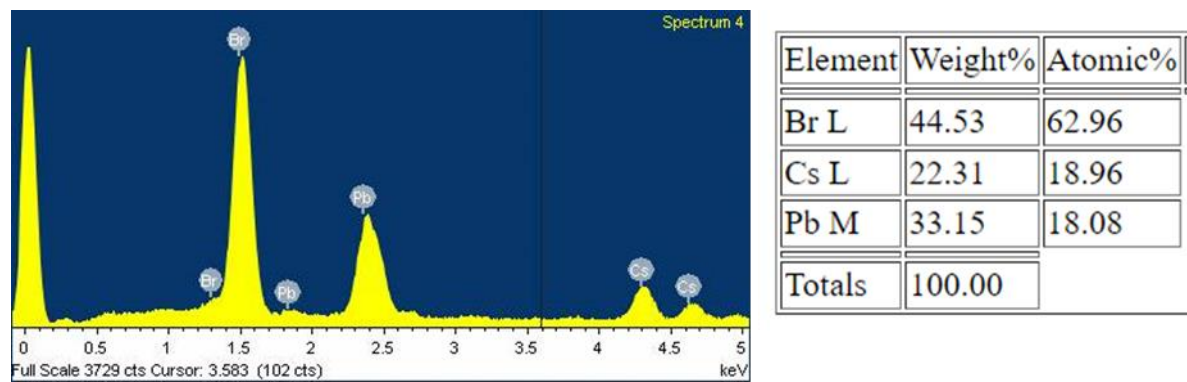


Fig S12. EDX Spectrum of $\text{CsPbBr}_3\text{-}4$ and quantitative analysis of the powder.